Hindawi
Mathematical Problems in Engineering
Volume 2022, Article ID 3145402, 18 pages
https://doi.org/10.1155/2022/3145402

Research Article

Condition Monitoring of Mechanical Components Based on MEMED-NLOPE under Multiscale Features

Xuan Wang,[1] **Bo She**,[1] **Zhangsong Shi**,[1] **Shiyan Sun**,[1] **and Fenqi Qin**[2]

[1]*Department of Weaponry Engineering, Naval University of Engineering, Wuhan 430033, China*
[2]*713 Research Institute of China Shipbuilding, Zhenzhou 450000, China*

Correspondence should be addressed to Bo She; she1611@126.com

Received 28 February 2022; Accepted 18 March 2022; Published 11 April 2022

Academic Editor: Ke Feng

An increasing popularity of researches focuses on the vibration signal with the characteristics of nonstationary, nonlinear, and strong noise interference. A nonlinear dimension and feature reduction method called multiple empirical mode entropy decomposition-nonlocal orthogonal preserving embedding (MEMED-NLOPE) is proposed to implement condition monitoring in this paper. Different from multiple empirical mode decomposition (MEMD), MEMED adopts maximum entropy method, which can directly output the subsignal with the maximum correlation and realize nonlinear dimensionality reduction. Besides, multiscale feature extraction method is used during preprocessing nonlinear data process, which realizes feature reduction. Finally, nonlocal orthogonal preserving embedding algorithm-exponentially weighted moving average (NLOPE-EWMA) realizes the automatic detection of the fault. Taking the laboratory rolling bearing test and naval gun pendulum mechanism test as cases, the effectiveness of MEMED-NLOPE is verified.

1. Introduction

Mechanical components as the vital parts of mechanical equipment are prone to wear and cracks on the surface with long-term overload operation. Wear increases the mechanical components transmission error, generally resulting in increased vibration, noise, and dynamic loads [1]. If the early minor damage of components cannot be detected in time, once the fatigue deteriorates and the parts break, the mechanical equipment will be shut down. With the deterioration of the fault degree, the mechanical equipment may be shut down for a long time, resulting in catastrophic failures and unexpected economic losses [2]. Therefore, condition monitoring of mechanical components is an effective measure to avoid the continuous deterioration of parts after damage. Vibration signals are widely used to characterize the state of mechanical equipment because of their ease of acquisition, but usually the collected vibration signals have many interference components and have nonstationary and nonlinear characteristics, which also bring difficulties to fault diagnosis.

In recent years, the multivariate statistical process monitoring (MSPM) technology is often used to detect faults in industrial production processes, such as partial least squares (PLS) [3], principal component analysis (PCA) [4], and independent component analysis (ICA) [5]. Those traditional monitoring methods process the intermediate data by dimensionality reduction and extract a small number of components to construct the monitoring statistics that can reflect the characteristics of the original data. At this time, the performance of dimensionality reduction will affect the monitoring effect.

Different from the dimensionality reduction method that maintains the global data structure, manifold learning is used to maintain the characteristics of local data structure, such as locally linear embedding (LLE) [6], Laplacian eigenmap (LE) [7], local preserving projections (LPP) [8], and neighborhood preserving embedding (NPE) [9]. Both LPP and NPE belong to linear projection methods, but these methods may lose the key information contained in the global data structure because they only consider the neighborhood relationship to maintain the local

characteristics. Therefore, in order to consider the global and local data structure characteristics, a method combining LPP and PCA method is proposed [10, 11]. The test results show that its monitoring performance is better than that of single method. Besides, orthogonal neighborhood preserving embedding (ONPE) is developed from NPE [12]; by setting additional orthogonal constraints on the projection vector, it not only maintains the characteristics of local structure but also avoids the distortion defects of NPE [13]. In order to fully consider the global and local structure characteristics of data, combined with the basic principles of PCA and ONPE algorithm, a nonlocal orthogonal preserving embedding (NLOPE) algorithm is proposed [14]. However, those methods still belong to linear method and have limitations in dealing with nonlinear data.

In the data preprocessing stage, empirical mode decomposition (EMD) is often used to describe the characteristics of nonlinear and nonstationary signals [15]. However, when processing multiple signals (multichannel signals), EMD may lead to different number and frequency scale of IMF for signal decomposition of each channel [16]. The proposal of multivariate empirical mode decomposition (MEMD) [17] ensures the matching of IMF components in quantity and scale. However, in the process of data preprocessing, the dimension of subsignals and features may increase, which will affect the effect of condition monitoring. To realize subsignals and nonlinear dimensionality reduction, entropy has been widely developed and used in this field, which can measure the correlation, uncertainty, and complexity of signals and features [18, 19].

In this paper, a linear dimension and feature reduction method called multiple empirical mode entropy decomposition-nonlocal orthogonal preserving embedding (MEMED-NLOPE) is proposed on the basis of MEMD and NLOPE. To reduce the redundancy of subsignal set and reduce the complexity of the system, MEMED takes both advantages of MEMD and maximum entropy method into account. To verify the effectiveness of MEMED-NLOPE, MEMED-NLOPE and MEMD-NLOPE are employed to detect the faults of naval gun pendulum mechanism, and MEMED-NLOPE is verified by the experimental data set of rolling bearing in laboratory.

The rest of the paper is organized as follows. MEMD, PCA, ONPE, and NLOPE are reviewed and analyzed in Section 2. The proposed MEMED-NLOPE is developed in Section 3. In Section 4, two cases are used to demonstrate the effectiveness of the proposed method. Finally, conclusions are drawn in Section 5.

2. Background Techniques

2.1. MEMD. EMD is suitable for one-dimensional real signals. For the processing of multichannel signals (multichannel signals), the EMD method often needs to solve the single channel signals, respectively, which may lead to the different number and frequency scale of IMF decomposed by each channel signal; that is, there is the problem of oscillation mode calibration of different channels, which is not conducive to the synchronous correlation analysis between multichannel signal channels. Although CMED [20], BEMD [21], and TEMD [22] are Multivariate Applications of EMD methods in multivariate data, they are limited to multivariate data: only binary and ternary signals. For real multivariate signals, it is still impossible to decompose the signal on the premise of correctly analyzing the physical meaning of the signal. The proposal of MEMD realizes the multichannel synchronous joint analysis of multichannel signal oscillation modes, obtains the common modes of different channels, ensures the matching of intrinsic mode function (IMF) components in quantity and scale, and solves the problem of mode calibration of multichannel signals.

The specific implementation of MEMD can be summarized as the following steps.

Let an n-dimensional vector group sequence $\{V(t)\}_{t=1}^{T} = \{v_1(t), v_2(t), \ldots, v_n(t)\}$ represent a n-tuple signal, the length of the signal sequence is T, and $X^{\theta_k} = \{x_1^k, x_2^k, \ldots, x_n^k\}$ represents the direction vector set of the corresponding angle $\theta^k = \{\theta_1^k, \theta_2^k, \ldots, \theta_{n-1}^k\}$ on the $n-1$-dimensional sphere. If you want to establish K direction vectors in spherical space, then $k = 1, 2, 3, \ldots, K$.

(1) The Hammersley sequence sampling method is used to obtain a suitable set of uniform sampling points on the $n-1$-dimensional sphere, that is, the direction vector of the n-dimensional space.

(2) The mapping $p^{\theta_k}(t)$ of the input signal $v(t)$ on each direction vector X^{θ_k} is calculated.

(3) Determine the instantaneous time $\{t^{\theta_k}\}_{k=1}^{K}$ corresponding to the extreme value of the mapping signal $\{p^{\theta_k}(t)\}_{k=1}^{K}$ of all direction vectors, and l represents the extreme point position, $l \in [1, T]$.

(4) The extreme point $[t_l^{\theta_k}, v(t_l^{\theta_k})]$ is interpolated by multivariate spline interpolation function to obtain K multivariate envelopes $\{e^{\theta_k}(t)\}_{k=1}^{K}$.

(5) For K direction vectors in spherical space, the mean $m(t)$ of n-tuple signal is as follows:

$$m(t) = \frac{1}{K} \sum_{K=1}^{K} e^{\theta_k}(t). \tag{1}$$

(6) Extract the intrinsic mode function $h(t)$ through $h(t) = v(t) - m(t)$. If $h(t)$ meets the judgment standard of multivariate IMF, take the $v(t) - h(t)$ result as the input signal in step (2), continue the iterative calculation in steps (2)~(6), and extract a new multivariate IMF component $h(t)$; otherwise, take $h(t)$ as the input signal of step (2) and continue the iteration of steps (2)~(6).

After a series of MEMD decomposition processes, similar to the EMD algorithm, the original n-tuple signal $\{V(t)\}_{t=1}^{T} = \{v_1(t), v_2(t), \ldots, v_n(t)\}$ is decomposed into a series of addition forms of IMF $(h_i(t)\}_{i=1}^{q})$ and Residual $r(t)$, as follows:

$$V(t) = \sum_{i=1}^{q} h_i(t) + r(t), \tag{2}$$

where q represents the decomposed multivariate IMF function, $h(t)$ is $\{h_i^1(t), h_i^2(t), \ldots, h_i^n(t)\}_{t=1}^T$, $r(t)$ is $\{r^1(t), r^2(t), \ldots, r^n(t)\}_{t=1}^T$, corresponding to n groups of IMF components and n margins of n-tuple signals, respectively. The number of IMF decomposed by each channel of multivariate signal is the same, and the frequencies of IMF in each layer are different. The first decomposed IMF frequency is high, and then the decomposed IMF frequency is low, and the decomposed residual frequency is the lowest. The IMF corresponding to each variable of n-tuple signal is aligned according to the frequency scale in n channels to form multiple IMF.

2.2. Principal Component Analysis. PCA, namely, principal component analysis, is one of the most widely used data dimensionality reduction algorithms. In this study, the PCA algorithm is implemented based on eigenvalue decomposition covariance matrix. The specific steps are as follows:

Step 1: input data set $X = \{x_1, x_2, x_3, \ldots, x_n\}$, which needs to be reduced to k dimension.

Step 2: deaveraging (i.e., decentralization), that is, each feature subtracts its own average.

Step 3: calculate the covariance matrix $(1/n)XX^T$. Note: dividing or not dividing the number of samples n or $n-1$ has no effect on the calculated eigenvector.

Step 4: find the eigenvalue and eigenvector of covariance matrix $(1/n)XX^T$ by eigenvalue decomposition method.

Step 5: sort the eigenvalues from large to small, and select the largest k of them. Then, the corresponding x eigenvectors are used as row vectors to form the eigenvector matrix P.

Step 6: convert the data into a new space constructed by k eigenvectors, i.e., $Y = PX$.

2.3. Orthogonal Neighborhood Preserving Embedding. Given data set $X = \{x_1, x_2, \ldots, x_N\} \in R^m$, as a kind of linear dimensionality reduction method, the goal of the orthogonal neighborhood preserving embedding (ONPE) algorithm is to reduce the dimension of high-dimensional data X to low-dimensional data $Y = \{y_1, y_2, \ldots, y_N\} \in R^d$, that is, $Y = A^T X$, using a transformation matrix $A = [a_1, a_2, \ldots, a_d] \in R^{m \times d}$ $(d < m)$, and the low-dimensional data can express the essential characteristics of the original high-dimensional data. The NPE algorithm is the basic form of ONPE. NPE maintains the local characteristics in the data structure by constructing the neighborhood graph between adjacent samples. Therefore, each sample can be expressed as a linear combination of adjacent samples and their corresponding weight coefficients. The weight coefficient matrix W minimizes the following objective functions:

$$\min \sum_i \left\| x_i - \sum_j W_{ij} x_j \right\|^2. \tag{3}$$

In order to fully maintain the local characteristics of the data structure, the high-dimensional spatial data x_i are mapped to the low-dimensional feature space to obtain y_i, and the weight coefficients between x_i and its nearest neighbors will be projected to the low-dimensional feature space to be saved to characterize the connection relationship between y_i and its nearest neighbors. The low-dimensional mapping Y of high-dimensional data X can calculate the following loss functions:

$$\begin{cases} \min \quad \sum_i \left\| y_i - \sum_j W_{ij} y_j \right\|^2, \\ \text{s.t.} \quad Y^T Y = A^T X X^T A = I, \end{cases} \tag{4}$$

where $\sum_{j=1}^k W_{ij} = 1$, $i = 1, 2, \ldots, N$, k is the number of nearest neighbors in the neighborhood of x_i. If x_j is not the nearest neighbor of x_i, there is $W_{ij} = 0$.

ONPE adds an orthogonal constraint on the basis of NPE, that is, mapping high-dimensional data to low-dimensional feature space through an orthogonal projection matrix A. According to (3) and (4), the projection matrix is calculated by the following formulas:

$$\begin{cases} a_1 = \arg\min_a \sum_i \left\| y_i - \sum_j W_{ij} y_j \right\|^2 = \arg\min_a A^T X M X^T A, \\ \text{s.t.} A^T X X^T A = I, \end{cases}$$

$$\begin{cases} a_k = \arg\min_a \sum_i \left\| y_i - \sum_j W_{ij} y_j \right\|^2 = \arg\min_a A^T X M X^T A, \\ \text{s.t.} a_k^T a_1 = a_k^T a_2 = \cdots = a_k^T a_{k-1} = 0, \\ A^T X X^T A = I, \end{cases} \tag{5}$$

where $k = 2, 3, \ldots, d$, $M = (I - W)^T (I - W)$. Through iterative calculation by Lagrange operator, the expression of orthogonal matrix A is as follows:

(a) a_1 is the eigenvector corresponding to the minimum eigenvalue of matrix $(XX^T)^{-1} XMX^T$;

(b) a_k is the eigenvector corresponding to the minimum eigenvalue of matrix $Q^{(k)}$, where $Q^{(k)}$ is

$$Q^{(k)} = \left\{ I - \left(XX^T\right)^{-1} A^{(k-1)} \left[\left(A^{(k-1)}\right)^T \left(XX^T\right)^{-1} A^{(k-1)} \right]^{-1} \left(A^{(k-1)}\right)^T \right\} \cdot \left(XX^T\right)^{-1} XMX^T, \tag{6}$$

where $A^{(k-1)} = [a_1, a_2, \ldots, a_{k-1}]$.

2.4. Objective Function of Nonlocal Orthogonal Preserving Embedding. In order to fully consider the global and local structure characteristics of data, combined with the basic principles of PCA and ONPE algorithm, a nonlocal orthogonal preserving embedding (NLOPE) algorithm is proposed. Assuming data set $x = \{x_1, x_2, \cdots, x_N\} \in R^{m\times N}$, the objective function of NLOPE is as follows:

$$\begin{aligned} J(a)_{\text{NLOPE}} &= \eta J(a)_{\text{Local}} - (1-\eta) J(a)_{\text{Global}} \\ &= \eta \min_a a^T x M x^T a - (1-\eta) \max_a a^T C a \\ &= \min_a a^T \left(\eta x M x^T - (1-\eta) C\right) a \\ &= \min_a a^T \left(\eta L' - (1-\eta) C\right) a, \end{aligned} \tag{7}$$

$$\text{s.t. } a_k^T a_1 = a_k^T a_2 = \cdots = a_k^T a_{k-1} = 0,$$
$$a^T \left[\eta x x^T + (1-\eta) I\right] a = 1, \tag{8}$$

where $C = (1/N)\sum_{i=1}^{N} (x_i - \overline{x})(x_i - \overline{x})^T$, $\overline{x} = (1/N)\sum_{i=1}^{N} x_i$.

Using Lagrange operator, projection matrix A can be obtained by calculating the following feature decomposition problem:

(a) a_1 is the eigenvector corresponding to the minimum eigenvalue of matrix $S^{-1}D$;

(b) a_k is the eigenvector corresponding to the minimum eigenvalue of matrix $Q^{(k)}$, where $Q^{(k)}$ is

$$Q^{(k)} = \left\{ I - (S)^{-1} a^{(k-1)} \left[\left(a^{(k-1)}\right)^T (S)^{-1} a^{(k-1)} \right]^{-1} \left(a^{(k-1)}\right)^T \right\} S^{-1} D, \tag{9}$$

where $k = 2, 3, \ldots, d$, d is the dimensions of data in NLOPE feature space, $+\ a^{(k-1)} = [a_1, a_2, \ldots, a_{k-1}]$, $S = \eta x x^T + (1-\eta) I$, and $D = \eta x M x^T - (1-\eta) C$.

For the new sample x_{new}, the mapping in the low-dimensional NLOPE feature space is

$$y_{\text{new}} = A^T x_{\text{new}}, \tag{10}$$

where $A = [a_1, a_2, \ldots, a_k]$.

The detailed derivation and calculation of projection matrix A are shown in [12]; there is

$$\left\{ I - S^{-1} a^{(k-1)} \left[\left(a^{(k-1)}\right)^T S^{-1} a^{(k-1)} \right]^{-1} \left(a^{(k-1)}\right)^T \right\} S^{-1} D a_k = \lambda a_k. \tag{11}$$

Thus, a_k is the eigenvector corresponding to the minimum eigenvalue of matrix $Q^{(k)}$, and the expression of $Q^{(k)}$ is as follows:

$$Q^{(k)} = \left\{ I - (S)^{-1} a^{(k-1)} \left[\left(a^{(k-1)}\right)^T (S)^{-1} a^{(k-1)} \right]^{-1} \left(a^{(k-1)}\right)^T \right\} S^{-1} D. \tag{12}$$

2.5. Calculation of Parameters. In the construction of the NLOPE model, parameter η makes the global data structure characteristics and local data structure characteristics occupy different components in the above model. The selection of parameter η affects the extraction of potential features in the data and then affects the effect of mechanical equipment fault detection, fault detection, and degradation performance evaluation.

It can be seen from (12) that the objective function of NLOPE is composed of two subobjective functions. Therefore, the objective function optimization problem of the NLOPE model is essentially a double objective optimization problem. Usually, it is difficult to obtain the optimal solution of the two subobjective functions at the same time. However, by balancing the two subobjective functions, a relatively better solution can be obtained.

By balancing the global data structure characteristics and local data structure characteristics of the model, the calculation of parameter η is as follows:

$$\eta S_{\text{Local}} = (1-\eta) S_{\text{Global}}, \tag{13}$$

where $S_{\text{Global}} = \rho(C)$ and $S_{\text{Local}} = \rho(L')$ represent the energy changes of $J(a)_{\text{local}}$ and $J(a)_{\text{local}}$, respectively.

According to (7), parameter η is used to balance matrix L' and matrix C in the NLOPE model, which can be regarded as the energy change of balance L' and C. Based on the principle of the PCA method, the eigenvectors corresponding to the first few large eigenvalues can characterize the distribution of matrix energy. Therefore, the maximum eigenvalues of matrix L' and matrix C can be used to estimate the energy change.

In the NLOPE model, parameter η is calculated as follows:

$$\eta = \frac{\rho(C)}{\rho(L') + \rho(C)}, \tag{14}$$

where $\rho(\cdot)$ is the spectral radius of the matrix, and matrix L' and matrix C are defined in (7).

2.6. Detection Index. Hotelling's T^2 and *SPE* statistics are often used as indicators of industrial process fault detection to judge whether the production process is abnormal. Hotelling's T^2 is used to measure the change of sample variables in the potential variable space, and *SPE* is mainly used to measure the change of sample variables in the residual space. When the statistics T^2 or *SPE* exceed their respective control limits, it indicates that the process may be abnormal. T^2 and *SPE* are calculated as follows:

$$T^2 = y^T \Lambda^{-1} y, \tag{15}$$

where y is the low-dimensional feature sample of sample x projected in NLOPE feature space, and $\Lambda = (yy^T/(N-1))$ is the covariance matrix of the projection vector of training sample in NLOPE feature space.

$$\begin{aligned} SPE &= \langle \Phi(x), \Phi(x) \rangle - \langle y, y \rangle \\ &= k(x,x) - \frac{2}{N}\sum_{i=1}^{N} k(x_i, x) + \frac{1}{N^2}\sum_{i=1}^{N}\sum_{j=1}^{N} k\left(x_i, x_j\right) - y^T y \\ &= 1 - \frac{2}{N}\sum_{i=1}^{N} k(x_i, x) + \frac{1}{N^2}\sum_{i=1}^{N}\sum_{j=1}^{N} k\left(x_i, x_j\right) - y^T y. \end{aligned} \tag{16}$$

Among them, $y_{\text{new}} = A^T x_{\text{new}}$.

In order to detect the early faults of mechanical equipment more accurately and reliably, the exponential weighted moving average (EWMA) is proposed by integrating T^2 and SPE statistics. The statistic U is a linear combination of T^2 and SPE statistics, including

$$U = \frac{T^2}{LT_2} + \frac{SPE}{L_{SPE}}, \tag{17}$$

where L_{T^2} and L_{SPE} are the control limits of statistics T^2 and SPE, respectively, which can be calculated by kernel density estimation (KDE). (T^2/L_{T^2}) and (SPE/L_{SPE}) normalize T^2 and SPE to (0, 1), respectively.

The detection index $EWMA$ is calculated as follows:

$$W_t = (1-\gamma)W_{t-1} + \gamma U_t, \tag{18}$$

where W_t represents the detection index, which is composed of the current index quantity and the historical index quantity, and γ is the smoothing coefficient between (0, 1). When γ takes a larger value, the current detection quantity U_t has a larger proportion in the detection quantity W_{t-1} than the historical detection quantity W_t. The control limit of the detection amount $EWMA$ is also calculated by the kernel density estimation method. In this chapter, the smoothing coefficient γ takes the empirical value of 0.2.

3. Proposed Condition Monitoring Model

Based on the analysis of the above background techniques, the MEMED-NLOPE model is proposed. Firstly, the architecture of MEMED-NLOPE is proposed; secondly, the preprocessing stage of nonlinear data is described in detail; finally, the steps of the automatic fault detection model based on NLOPE-EWMA is described.

3.1. Proposed Architecture. The MEMED-NLOPE model is mainly divided into two parts. The first part is nonlinear data preprocessing, and the second part is automatic fault detection model.

For the first part, MEMED decomposes the signals collected by each sensor, quantitatively analyzes the correlation and orthogonality between the multiscale subsignal and the original signal, selects the subsignal with the maximum correlation for the preliminary extraction of multi domain features, and uses the feature measurement criterion based on mutual information to optimize and eliminate redundant features, as the input of the fault detection model.

For the second part, it proposes condition monitoring model, adopts PCA which extracts the correlation between multidimensional variables from the historical normal operation data, and diagnoses abnormalities through their unexpected changes, but PCA only considers the global structure relationship between samples and ignores the local structure relationship. Therefore, based on the PCA multivariate statistical process monitoring method, combined with the local orthogonal preserving embedding (ONPE) algorithm, this project proposes NLOPE, which uses exponential weighted moving average (EWMA) statistics as detection index to realize the construction of the condition monitoring model. The research scheme is shown in Figure 1.

3.2. Preprocessing Nonlinear Data

3.2.1. MEMED

(1) Maximum Entropy Method. Based on the information entropy theory, the mutual information between different subsignals and source signals is measured to characterize the correlation of subsignals, reduce the redundancy of subsignal set, and reduce the complexity of the system. The formula of information entropy is as follows:

$$\begin{aligned} H(X) &= E[I(X)] \\ &= -\sum_{i=1}^{n} p(x_i) I(x_i) \\ &= -\sum_{i=1}^{n} p(x_i) \log_b p(x_i), \end{aligned} \tag{19}$$

where $I(x_i)$ represents the amount of information of x_i:

$$\begin{aligned} I(x_i) &= \log_b\left(\frac{1}{p(x_i)}\right) \\ &= -\log_b p(x_i). \end{aligned} \tag{20}$$

$p(x_i)$ is the probability of occurrence of x_i. The number of information ontologies contained in a randomly generated event is only related to the probability of occurrence of the event. The lower the probability of an event, the larger the information ontology contained in the received information when the event really occurs. The meaning is that the event with probability 0 has a large amount of information; on the contrary, it has a small amount of information. The reason for taking logarithm is to make the product sum. Two independent events x, y: $p(x,y) = p(x) * p(y)$ and $I(x,y) = I(x) + I(y)$.

Information entropy is the mathematical expectation of information.

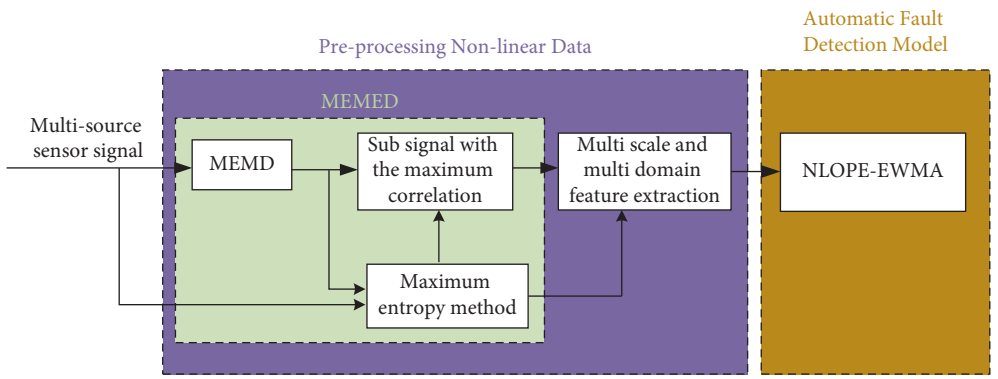

Figure 1: Research scheme of MEMED-NLOPE.

Mutual information is

$$I(x_i, y_i) = \log \frac{p(x_i, y_i)}{p(x_i)p(y_i)}. \quad (21)$$

Average mutual information is the mathematical expectation of mutual information:

$$I(X,Y) = E[I(x_i, y_i)] = \sum_i \sum_j p(x_i, y_i) \log \frac{p(x_i, y_i)}{p(x_i)p(y_i)}. \quad (22)$$

From the formula,

$$I(X,Y) = H(X) + H(Y) - H(X,Y). \quad (23)$$

(2) MEMED Flow Chart. Based on MEMD, MEMED adopts the maximum entropy method to output the subsignal with the maximum correlation, which realizes the function of dimension reduction and avoid data explosion. The specific flow of MEMD is shown in Figure 2.

3.2.2. Multiscale Feature Extraction Method

(1) Fault Feature Construction Method. The vibration signal is used to evaluate the running state of mechanical equipment. Generally, the corresponding features are extracted from the time domain, frequency domain, and time-frequency domain of the signal as the basis of diagnosis. Time-domain analysis is to describe the change of signal waveform and amplitude with time. Frequency domain analysis is to describe the change of signal power or energy with frequency. Time-frequency analysis is to study the change of signal spectrum with time and represent the distribution of signal strength or energy in both time and frequency dimensions.

Time-domain and frequency-domain features generally include root mean square, kurtosis, skewness, peak factor, spectral mean square deviation, and envelope spectral variance. Table 1 contains 11 times domain characteristic parameters ($p_1 - p_{11}$) and 13 frequency domain characteristic parameters ($p_{12} - p_{24}$). In each characteristic expression, $x(n)$ is the time-domain signal sequence, $n = 1, 2, \ldots, N$, N are the number of samples, $s(k)$ is the spectrum of signal $x(n)$, $k = 1, 2, \ldots, K$, K are the number of spectral lines, and f_k is the frequency value of the k spectral line. The time-domain characteristic parameters p_1 and $p_3 - p_5$ describe the amplitude and energy changes of the time-domain signal; p_2 and $p_6 - p_{11}$ describe the time series distribution of time-domain signals. The frequency domain characteristic parameter p_{12} describes the change of frequency domain energy; $p_{13} - p_{15}$, p_{17} and $p_{21} - p_{24}$ reflect the concentration and dispersion of the spectrum; p_{16}, $p_{18} - p_{20}$ reflects the change of the position of the main frequency band.

The time-frequency domain features include sample entropy, permutation entropy, wavelet energy entropy, and EEMD information entropy, which are generally calculated by time-frequency analysis methods such as wavelet analysis and empirical mode decomposition.

(2) Fault Feature Selection Method. Similarly, based on the information entropy theory, the mutual information between different features is measured to characterize the correlation between features and reduce the redundancy of feature sets.

3.3. Automatic Fault Detection Model Based on NLOPE-EWMA. The offline modeling steps based on NLOPE are as follows:

Step 1: the features of training samples after MEMD adaptive decomposition, multiscale subsignal selection, and multi-scale feature extraction are constructed as feature samples, and the feature samples are standardized

Step 2: calculate the projection coefficient matrix from (9)

Step 3: calculate the sum SPE statistics of all training samples, and calculate the sum of control limits, so as to calculate the detection index EWMA and its control limits

The steps of online detection based on NLOPE are as follows:

Step 1: after multiscale feature extraction, the feature samples of each test sample are constructed, and the feature test samples are standardized by using the mean and variance of the training feature samples

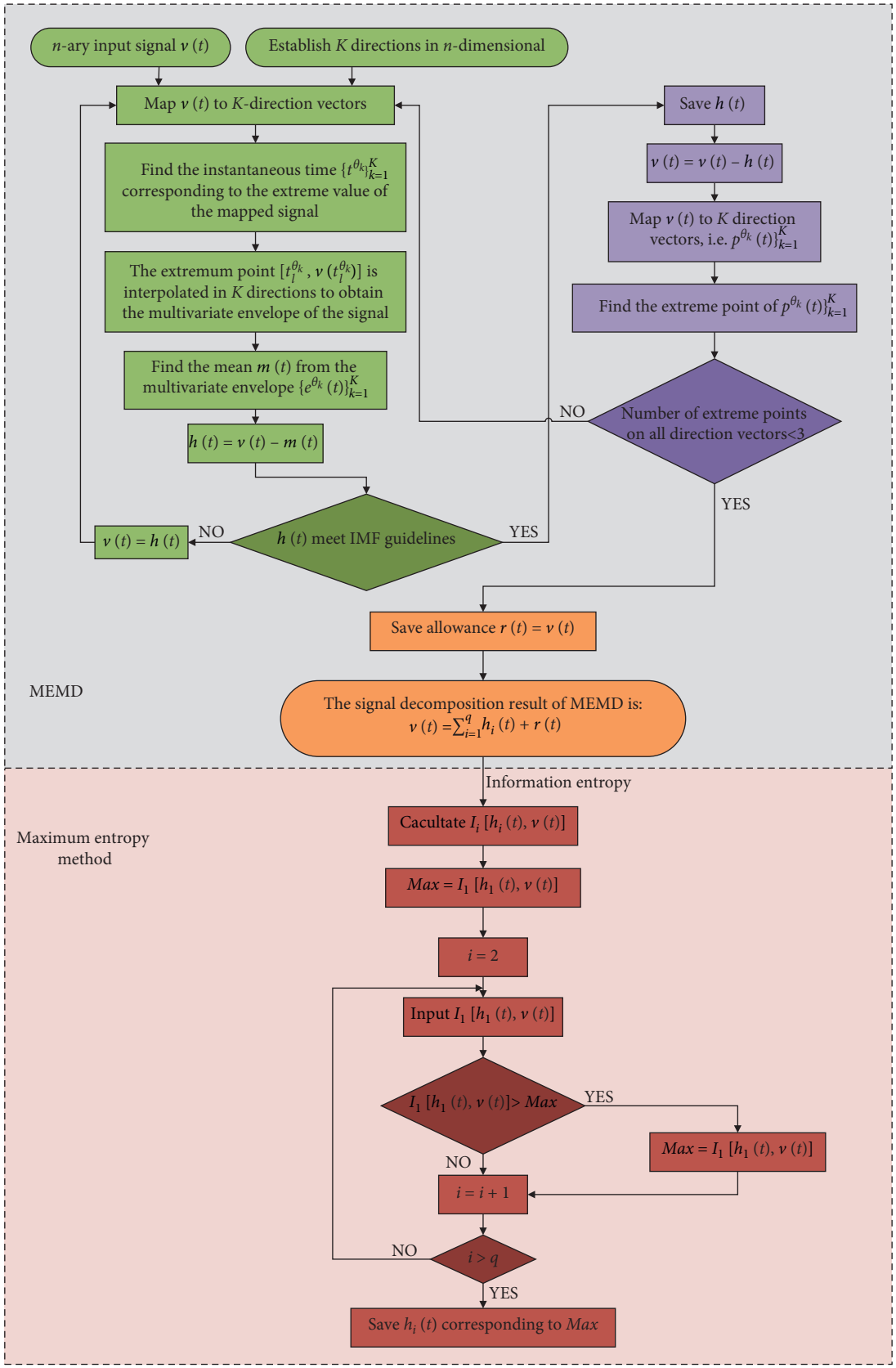

Figure 2: MEMED flow chart.

Table 1: Characteristic parameters.

No.	Characteristic expression	No.	Characteristic expression	No.	Characteristic expression
1	$p_1 = (\sum_{n=1}^{N} x(n)/N)$	9	$p_9 = (p_5/p_3)$	17	$p_{17} = \sqrt{\sum_{k=1}^{K} (f_k - p_{16})^2 s(k)/K}$
2	$p_2 = \sqrt{\sum_{n=1}^{N} (x(n) - p_1)^2/N - 1}$	10	$p_{10} = (p_4/1/N \sum_{n=1}^{N} \lvert x(n)\rvert)$	18	$p_{18} = \sqrt{\sum_{k=1}^{K} f_k^2 s(k)/\sum_{k=1}^{K} s(k)}$
3	$p_3 = (\sum_{n=1}^{N} \sqrt{\lvert x(n)\rvert}/N)^2$	11	$p_{11} = (p_5/1/N \sum_{n=1}^{N} \lvert x(n)\rvert)$	19	$p_{19} = \sqrt{\sum_{k=1}^{K} f_k^4 s(k)/\sum_{k=1}^{K} f_k^2 s(k)}$
4	$p_4 = \sqrt{\sum_{n=1}^{N} x(n)^2/N}$	12	$p_{12} = (\sum_{k=1}^{K} s(k)/K)$	20	$p_{20} = \sum_{k=1}^{K} f_k^2 s(k)/\sqrt{\sum_{k=1}^{K} s(k) \sum_{k=1}^{K} f_k^4 s(k)}$
5	$p_5 = \max\lvert x(n)\rvert$	13	$p_{13} = (\sum_{k=1}^{K} (s(k) - p_{12})^2/K - 1)$	21	$p_{21} = (p_{17}/p_{16})$
6	$p_6 = (\sum_{n=1}^{N} (x(n) - p_1)^3/(N-1)p_2^3)$	14	$p_{14} = (\sum_{k=1}^{K} (s(k) - p_{12})^3/K(\sqrt{p_{13}})^3)$	22	$p_{22} = (\sum_{k=1}^{K} (f_k - p_{16})^3 s(k)/K p_{17}^3)$
7	$p_7 = (\sum_{n=1}^{N} (x(n) - p_1)^4/(N-1)p_2^4)$	15	$p_{15} = (\sum_{k=1}^{K} (s(k) - p_{12})^4/K p_{13}^2)$	23	$p_{23} = (\sum_{k=1}^{K} (f_k - p_{16})^4 s(k)/K p_{17}^4)$
8	$p_8 = (p_5/p_4)$	16	$p_{16} = (\sum_{k=1}^{K} f_k s(k)/\sum_{k=1}^{K} s(k))$	24	$p_{24} = (\sum_{k=1}^{K} (f_k - p_{16})^{(1/2)} s(k)/K\sqrt{p_{17}})$

Step 2: calculate the projection of the test sample in the low-dimensional feature space from (10)

Step 3: calculate the detection amount EWMA corresponding to the test sample and judge whether it exceeds the monitoring limit

The fault detection process based on the NLOPE method is shown in Figure 3. Using the NLOPE method, the offline detection model is constructed by using normal vibration signals, the new data samples are input into the detection model, and the fault detection of mechanical equipment can be carried out by calculating the detection indexes.

4. Experimental Verification and Analysis

To verify the effectiveness of MEMED-NLOPE, the laboratory rolling bearing test and naval gun pendulum mechanism test are taken as cases. Besides, the programming software used in the experiment is MathWorks Matlab R2018a, and the computer configuration is Core i7-10875H CPU @ 2.30 GHz.

4.1. Experimental Data Set of Naval Gun Pendulum Mechanism

4.1.1. Experimental Design. The life test of typical mechanical parts of naval gun is carried out by using the test bench of energy storage mechanism of single 130 mm naval gun pendulum. In the test, the data of the health and fracture damage of the pressing plate and the health and crack damage of the roller are collected. The damage of mechanical parts is shown in Figures 4 and 5. In the test, six vibration acceleration sensors, numbered a1–a6, and acoustic sensors are arranged near the sliding plate and pressing plate mechanism of the pendulum. The location of the sensor measuring points is shown in Figure 6. Two vibration acceleration sensors (No. a7-a8) are arranged near the roller track, and the measuring point positions of the sensors are shown in Figures 7 and 8.

The test data collected are composed of the following:

(1) *Platen Data.* The composition of platen data collected in the test is shown in Table 2, and the sampling frequency is 10 kHz. The number of times of one test in the table indicates that the artillery test bench has completed a complete action cycle of latch closing, recoil, reentry, latch opening, lower swing, and upper swing.

(2) *Roller Data.* The roller test adopts rollers in two states, and the test data composition is shown in Table 3.

4.1.2. Condition Monitoring and Analysis of Pendulum Mechanism. MEMD-NLOPE and MEMED-NLOPE are used to monitor the condition of platen in different status, and the results are shown in Figure 9.

It can be seen from Figure 9 that under the condition monitoring model constructed by MEMD-NLOPE, when the monitoring object is the healthy platen and roller, some of the detection indicators of the test sample exceed the monitoring limit; the part exceeding the monitoring limit indicates that the detection model generates false alarm. While when the monitoring object is the platen and roller tending to be damaged, some of the detection indicators of the test sample are below the monitoring limit. Under the condition monitoring model constructed by MEMED-NLOPE, most of the detection indicators of the test samples are within the normal monitoring range, and the collected training samples are consistent with the state of the naval gun platform.

4.1.3. Summary. Through the action cycle test of mechanical mechanism on the naval gun test bench, the data information of key mechanical parts in the damaged state is obtained. Using the proposed detection model, the normal operation state and abnormal operation state of the naval gun test bench are detected and analyzed. The performance evaluation results based on MEMD-NLOPE and MEMED-NLOPE are shown in Table 4, respectively.

According to the results in Table 4, the performance of condition monitoring based on MEMED-NLOPE is better than that based on MEMD-NLOPE, and the average accuracy of normal and damage detection of platen and roller is greater than 90%, indicating that MEMED-NLOPE can determine the normal operation state of pendulum mechanism and detect the faults of mechanical components. However, when the platen is in a healthy state, the false

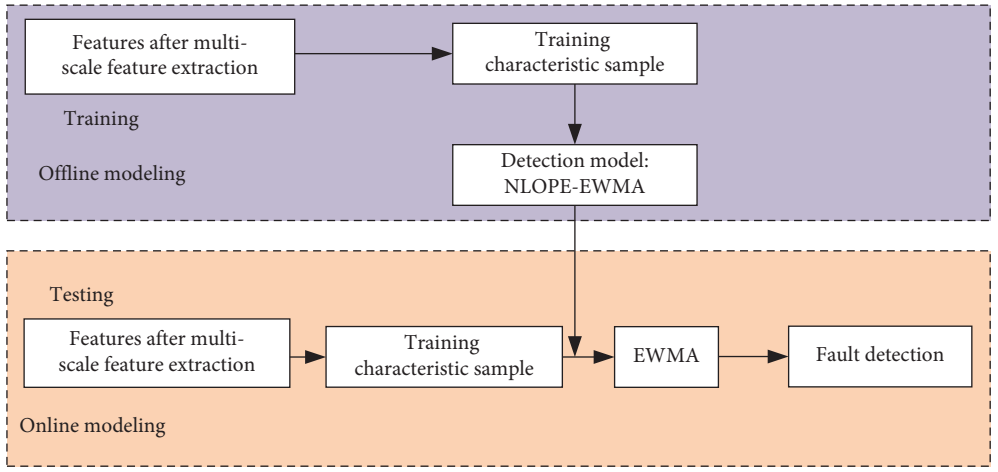

Figure 3: Fault detection process based on NLOPE-EWMA.

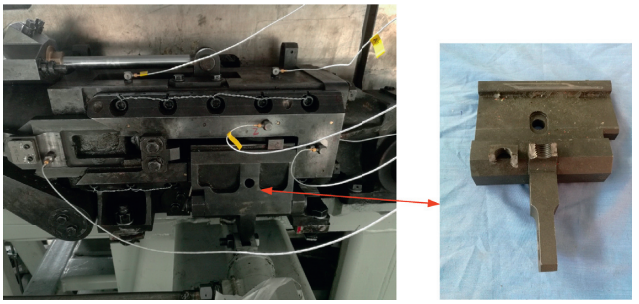

Figure 4: Damage diagram of pressing plate.

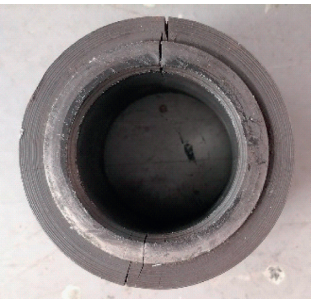

Figure 5: Crack damage of roller.

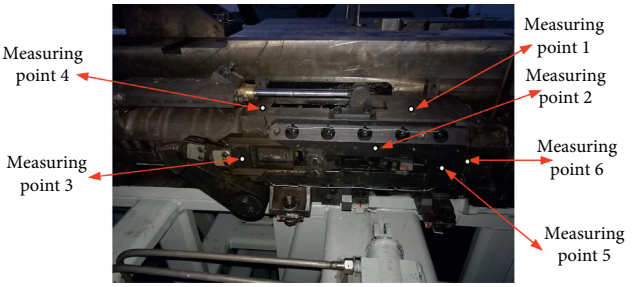

Figure 6: Layout of measuring points of acceleration sensor.

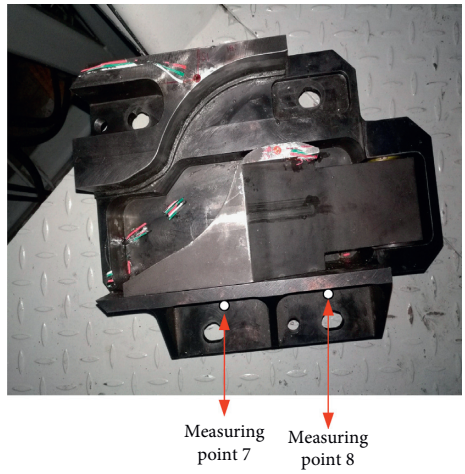

Figure 7: Layout of measuring points of acceleration sensor.

(a) (b)

Figure 8: Test bench sensor measuring points.

Table 2: Composition of platen test data.

No.	Data	Number of tests	Platen status	Data type
1	Yaban_Data1	20	Damaged status	Test data
2	Yaban_Data2	20	Damaged status	Test data
3	Yaban_Data3	20	Healthy status	Test data
4	Yaban_Data4	20	Healthy status	Test data
5	Yaban_Data5	20	Healthy status	Training data

Table 3: Composition of roller test data.

No.	Data	Number of tests	Roller status	Data type
1	Gunlun_Data1	20	Damaged status	Test data
2	Gunlun_Data2	20	Damaged status	Test data
3	Gunlun_Data3	20	Healthy status	Test data
4	Gunlun_Data4	20	Healthy status	Test data
5	Gunlun_Data5	20	Healthy status	Training data

alarm rate is little high, which reflects that MEMD-NLOPE has certain instability in this test.

4.2. Experimental Data Set of Rolling Bearing in Laboratory

4.2.1. Experimental Design. The mechanical failure test bench used in the laboratory is purchased from Anhui Chaokun Testing Equipment Co., Ltd. The test of bearing is shown in Figure 10.

The data used in the study are shown in Table 5.

4.2.2. Condition Monitoring and Analysis. MEMED-NLOPE is used to monitor the condition of bearing in different status, and the results are shown in

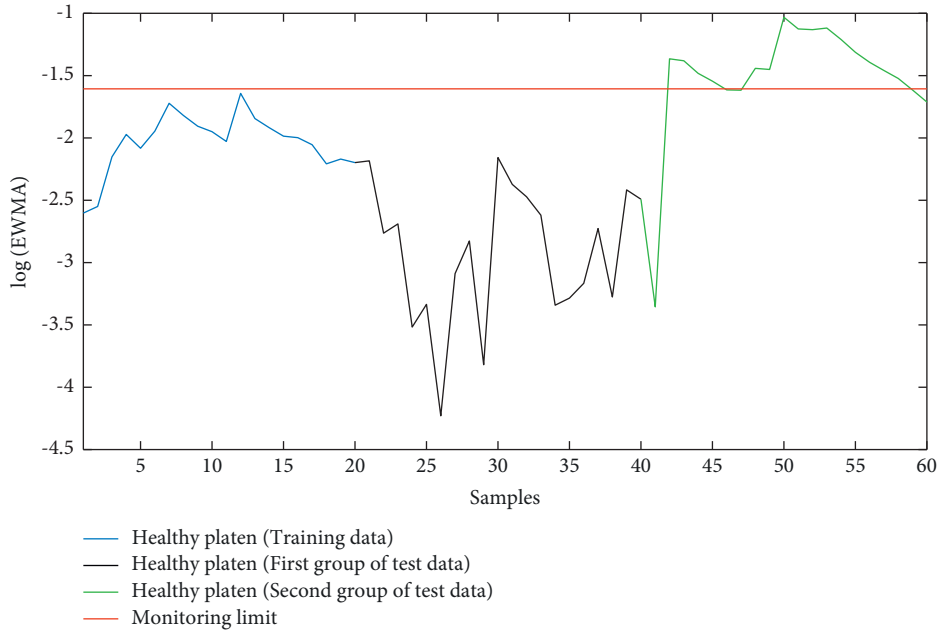

(a)

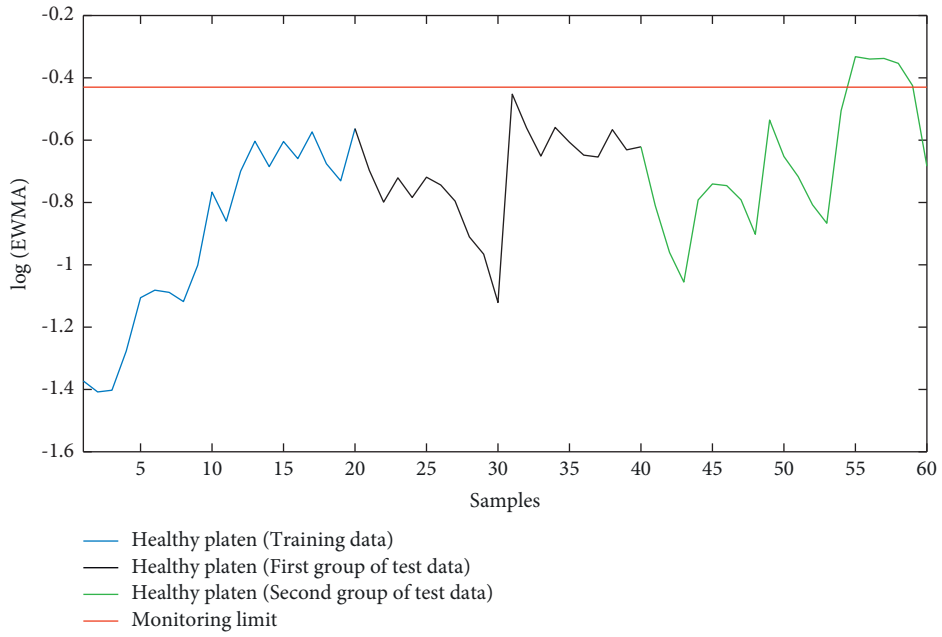

(b)

Figure 9: Continued.

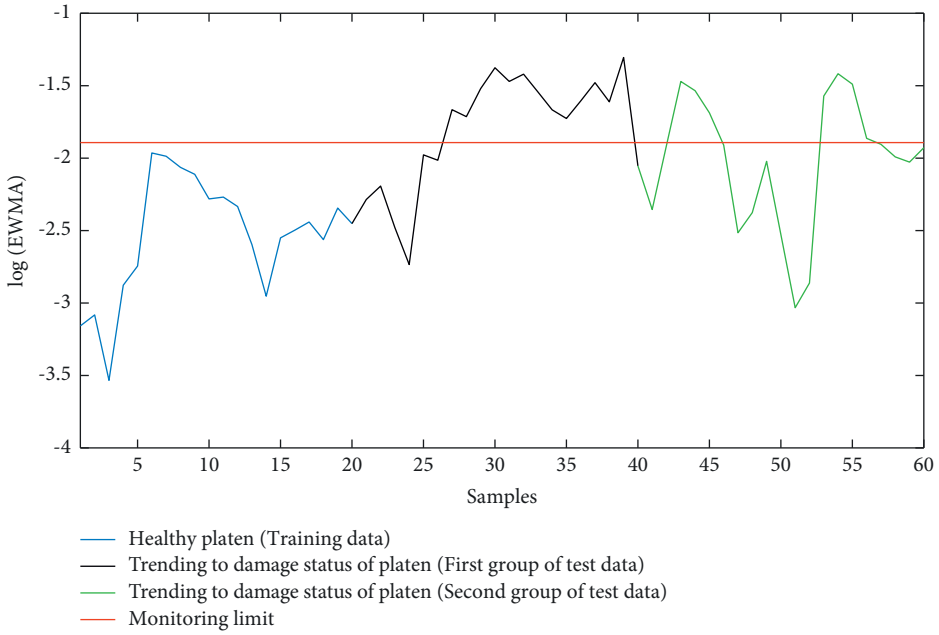

(c)

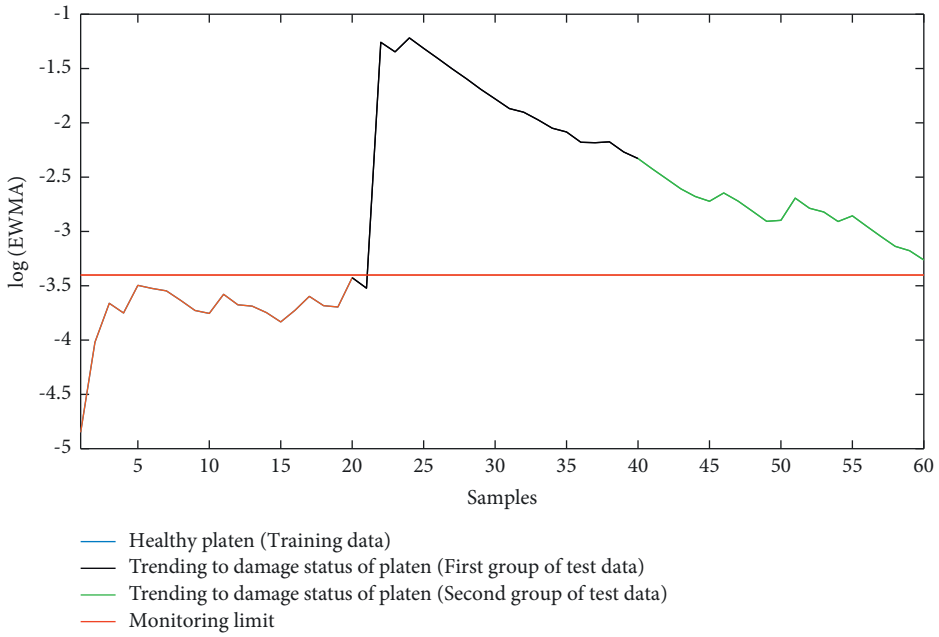

(d)

Figure 9: Continued.

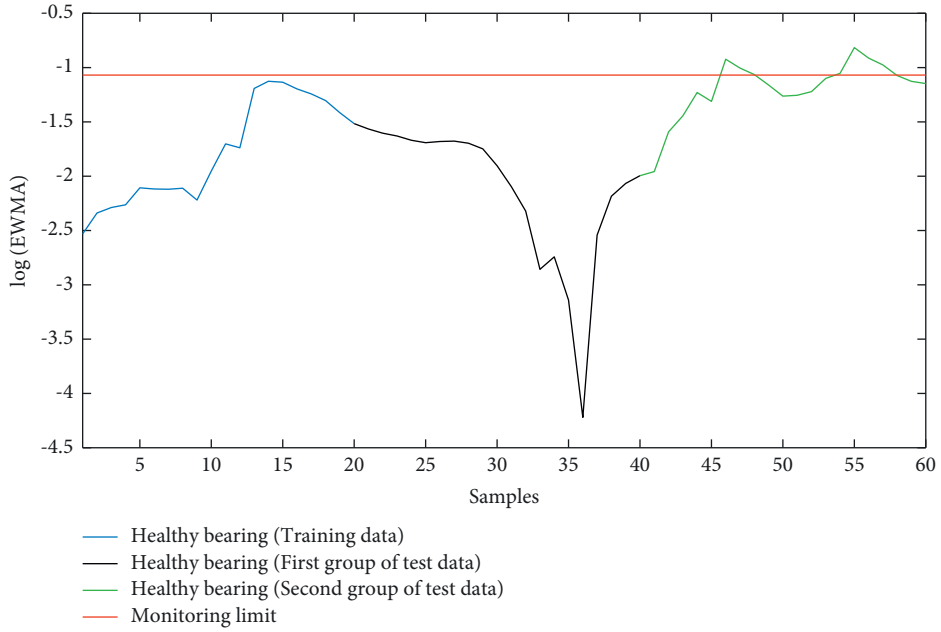

(e)

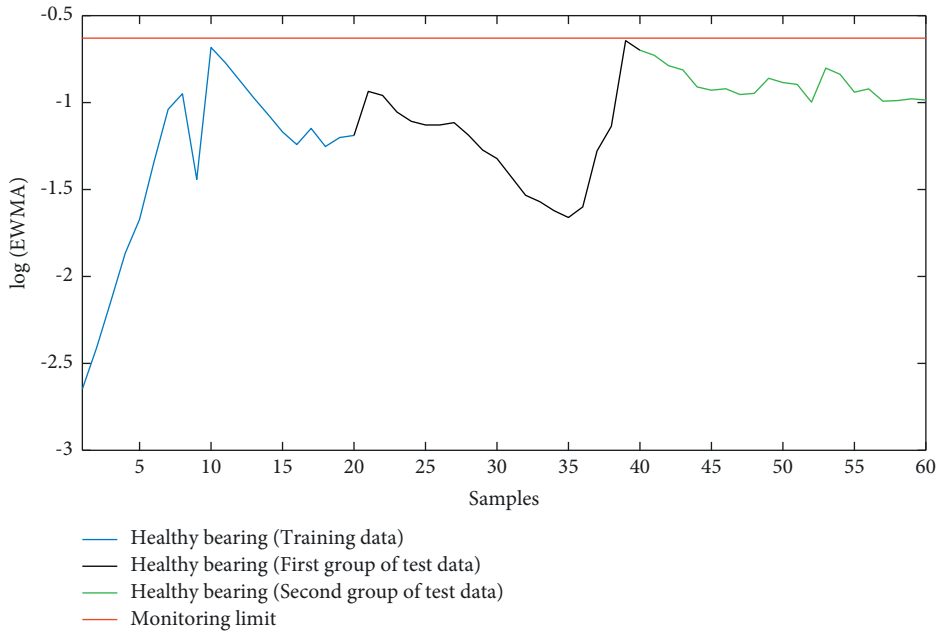

(f)

Figure 9: Continued.

(g)

(h)

Figure 9: Condition monitoring results using MEMD-NLOPE and MEMED-NLOPE. (a) Condition monitoring of healthy platen using MEMD-NLOPE. (b) Condition monitoring of healthy platen using MEMED-NLOPE. (c) Condition monitoring of trending to damage status of platen using MEMD-NLOPE. (d) Condition monitoring of trending to damage status of platen using MEMED-NLOPE. (e) Condition monitoring of healthy bearing using MEMD-NLOPE. (f) Condition monitoring of healthy bearing using MEMED-NLOPE. (g) Condition monitoring of concave crack on outer race of roller using MEMD-NLOPE. (h) Condition monitoring of concave crack on outer race of roller using MEMED-NLOPE.

Figure 11; the corresponding data of different test groups are as follows:

(a) Zc_Data1 (Taining data), Zc_Data2 (First group of test data), and Zc_Data3 (Second group of test data)

(b) Zc_Data1 (Training data), Zc_Data4 (First group of test data), and Zc_Data5 (Second group of test data)

(c) Zc_Data1 (Training data), Zc_Data6 (First group of test data), and Zc_Data7 (Second group of test data)

(d) Zc_Data1 (Training data), Zc_Data8 (First group of test data), and Zc_Data9 (Second group of test data)

(e) Zc_Data1 (Training data), Zc_Data10 (First group of test data), and Zc_Data11 (Second group of test data)

Table 4: Performance evaluation results based on MEMD-NLOPE and MEMED-NLOPE.

Mechanical parts	Status	Cumulative number of tests	False alarm times/ missed detection times based on MEMD-NLOPE	False alarm rate/ missed detection rate based on MEMD-NLOPE (%)	False alarm times/ missed detection times based on MEMED-NLOPE	False alarm rate/ missed detection rate based on MEMED-NLOPE (%)
Platen	Healthy status	40	15	37.50	4	10.00
	Tending to damaged status	40	19	47.50	1	2.50
Roller	Healthy status	40	6	15.00	0	0.00
	Damaged status	40	4	10.00	1	2.50

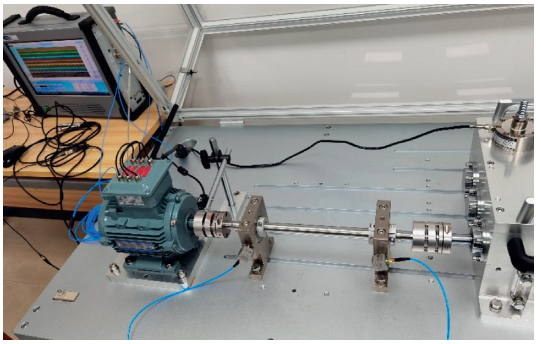

Figure 10: Mechanical failure test bench for bearing.

Table 5: Data related to mechanical failure test of bearing.

Experimental group	Rated speed	Fault design of bearing	Vibration signal data	Sampling frequency of vibration signal
Experimental group 1	1000 r/min	Healthy status	Zc_Data1—Zc_Data3	200 ks/S
Experimental group 2	1000 r/min	Inner race damaged status	Zc_Data4—Zc_Data5	200 ks/S
Experimental group 3	1000 r/min	Outer race damaged status	Zc_Data6—Zc_Data7	200 ks/S
Experimental group 4	1000 r/min	Ball damaged status	Zc_Data8—Zc_Data9	200 ks/S
Experimental group 5	1000 r/min	Mixed damaged status	Zc_Data10—Zc_Data11	200 ks/S

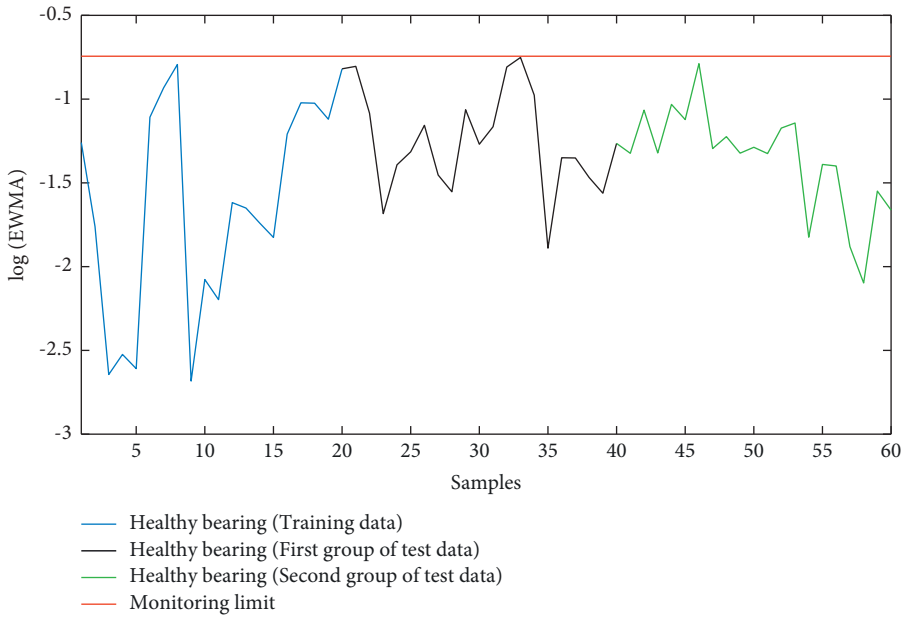

(a)

Figure 11: Continued.

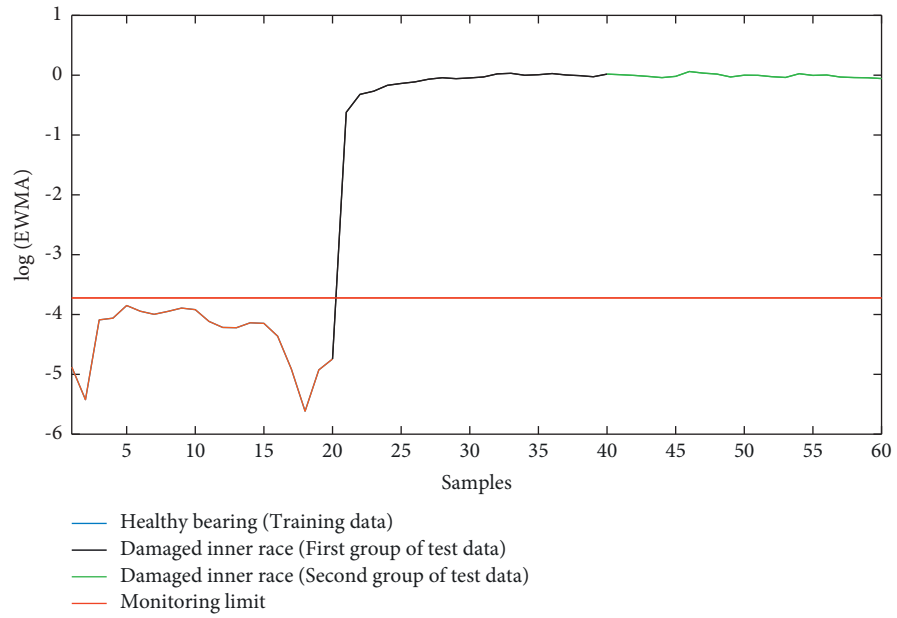

(b)

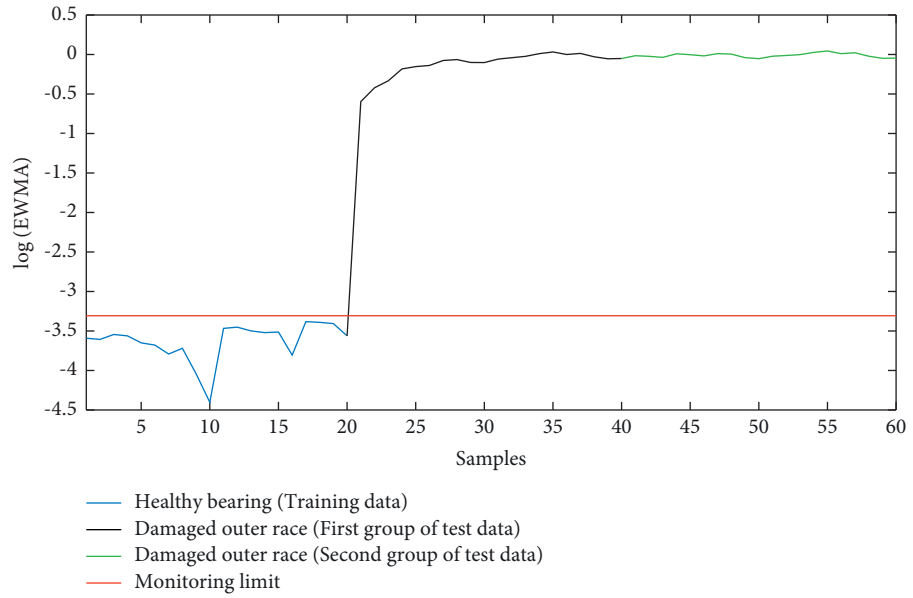

(c)

Figure 11: Continued.

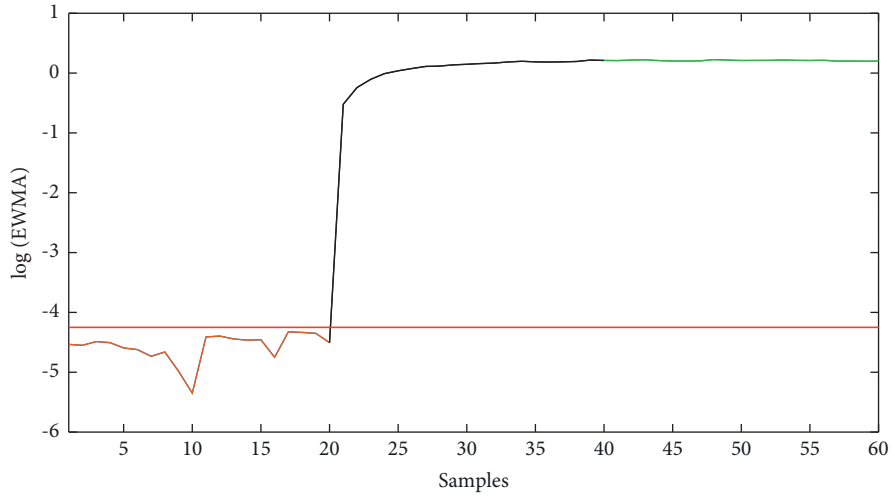

(d)

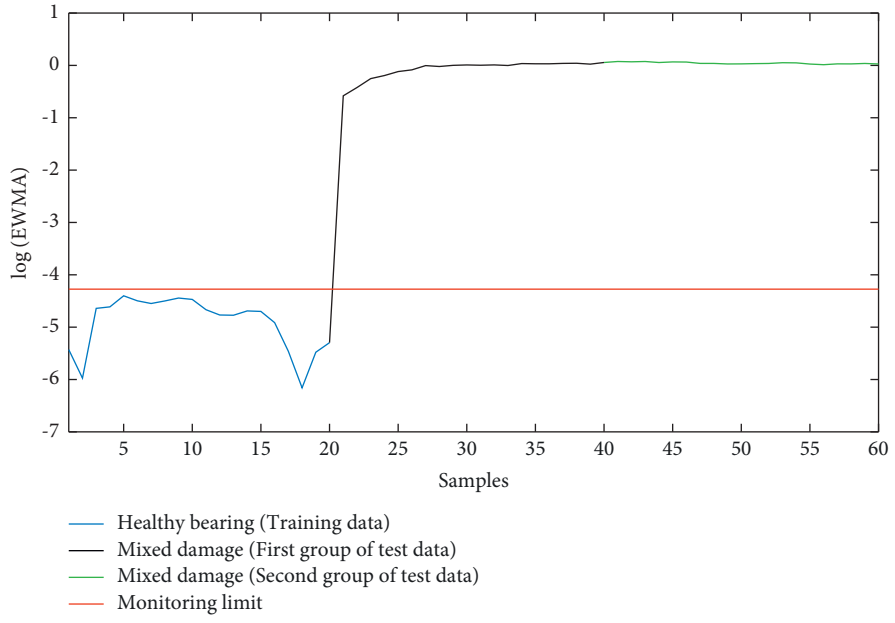

(e)

Figure 11: Condition monitoring of different states of bearings. (a) Condition monitoring of healthy bearing. (b) Condition monitoring of damaged inner race. (c) Condition monitoring of damaged outer race. (d) Condition monitoring of damaged ball. (e) Condition monitoring of mixed damage.

Table 6: Performance evaluation results of the fault detection model.

Status	Cumulative number of tests	False alarm times/missed detection times	False alarm rate/missed detection rate (%)
Healthy status	40	0	0.00
Inner damage	40	0	0.00
Outer damage	40	0	0.00
Ball damage	40	0	0.00
Mixed damage	40	0	0.00

4.2.3. Summary. Through the rolling bearing test on the mechanical fault test-bed in the laboratory, the data information of the bearing under different states is obtained, and the normal operation state and abnormal operation state of the bearing are detected and analyzed by using the proposed detection model. The performance evaluation results of MEMED-NLOPE are shown in Table 6.

It can be seen that MEMED-NLOPE can detect the bearing in different states, and its performance is verified.

5. Conclusions

In this paper, a linear dimension and feature reduction method called multiple empirical mode entropy decomposition-nonlocal orthogonal preserving embedding is proposed. In order to reduce the dimension of multivariate signals and consider the correlation between sub signals and source signals, MEMED adopts the maximum entropy method to directly output the subsignal with the maximum correlation. Then, the multiscale feature extraction method reduces the redundancy of feature set by describing the correlation between features. Finally, the automatic fault detection model based on NLOPE-EWMA is proposed to realize condition monitoring. Based on the results of two cases, the performance of condition monitoring based on MEMED-NLOPE is verified, in which the average accuracy of normal and damage detection is higher in comparison with MEMD-NLOPE. For the future work, the massive amounts of data from multiple sensors could be considered for naval gun in health condition monitoring and fault diagnostics.

Data Availability

The experimental data set of naval gun pendulum mechanism data and rolling bearing in laboratory used to support the findings of this study are available from the corresponding author upon request.

Conflicts of Interest

The authors declare that they have no conflicts of interest.

Acknowledgments

This research was supported by National Nature Science Foundation of China (nos. 61640308 and 61573364) and Nature Science Foundation of Naval University of Engineering (no. 20161579).

References

[1] K. Feng, P. Borghesani, W. A. Smith et al., "Vibration-based updating of wear prediction for spur gears," *Wear*, vol. 426-427, pp. 1410–1415, 2019.

[2] K. Feng, W. A. Smith, P. Borghesani, R. B. Randall, and Z. Peng, "Use of cyclostationary properties of vibration signals to identify gear wear mechanisms and track wear evolution," *Mechanical Systems and Signal Processing*, vol. 150, Article ID 107258, 2020.

[3] S. J. Qin, "Survey on data-driven industrial process monitoring and diagnosis," *Annual Reviews in Control*, vol. 36, no. 2, pp. 220–234, 2012.

[4] Q. Jiang, X. Yan, and B. Huang, "Performance-driven distributed PCA process monitoring based on fault-relevant variable selection and bayesian inference," *IEEE Transactions on Industrial Electronics*, vol. 63, no. 1, pp. 377–386, 2016.

[5] Z. Ge, "Review on data-driven modeling and monitoring for plant-wide industrial processes," *Chemometrics and Intelligent Laboratory Systems*, vol. 171, pp. 16–25, 2017.

[6] S. T. Roweis and L. K. Saul, "Nonlinear dimensionality reduction by locally linear embedding," *Science*, vol. 290, no. 5500, pp. 2323–2326, 2000.

[7] M. Belkin and P. Niyogi, "Laplacian eigenmaps for dimensionality reduction and data representation," *Neural Computation*, vol. 15, no. 6, pp. 1373–1396, 2003.

[8] X. He and P. Niyogi, "Locality preserving projections," *Advances in Neural Information Processing Systems*, vol. 16, pp. 153–160, 2004.

[9] X. He, D. Cai, S. Yan, and H. Zhang, "Neighborhood preserving embedding," in *Proceedings of the 10th IEEE International Conference on Computer Vision (ICCV '05)*, pp. 1208–1213, Beijing, China, October 2005.

[10] J. Yu, "Local and global principal component analysis for process monitoring," *Journal of Process Control*, vol. 22, no. 7, pp. 1358–1373, 2012.

[11] J. Wang, J. Feng, and Z. Y. Han, "Locally preserving PCA method based on manifold learning and its application in fault detection," *Control and Decision*, vol. 22, no. 5, pp. 683–687, 2013.

[12] X. Liu, J. Yin, Z. Feng, J. Dong, and L. Wang, "Orthogonal neighborhood preserving embedding for face recognition," in *Proceedings of the 14th IEEE International Conference on Image Processing, ICIP 2007*, pp. I133–I136, San Antonio, TX, USA, September 2007.

[13] D. Cai, X. He, J. Han, and H.-J. Zhang, "Orthogonal laplacianfaces for face recognition," *IEEE Transactions on Image Processing*, vol. 15, no. 11, pp. 3608–3614, 2006.

[14] B. She, F. Tian, W. Liang, and G. Zhang, "Nonlinear model for condition monitoring and fault detection based on nonlocal kernel orthogonal preserving embedding," *Shock and Vibration*, vol. 2018, no. 5, pp. 1–16, 2018.

[15] A. Dorostghol and M. Dorfeshan, "Intelligent fault diagnosis via EMD method," *Journal of Applied Sciences*, vol. 12, no. 18, pp. 1960–1965, 2012.

[16] D. Looney and D. P. Mandic, "Multiscale image fusion using complex extensions of EMD," *IEEE Transactions on Signal Processing*, vol. 57, no. 4, pp. 1626–1630, 2009.

[17] N. Rehman and D. P. Mandic, "Multivariate empirical mode decomposition," *Proceedings of the Royal Society A: Mathematical, Physical & Engineering Sciences*, vol. 466, no. 2117, pp. 1291–1302, 2010.

[18] J. Xu, M. Yuan, and Y. Ma, "Feature Selection Using Self-Information and Entropy-Based Uncertainty Measure for Fuzzy Neighborhood Rough Set," *Complex & Intelligent Systems*, pp. 1–19, 2021.

[19] Y. Li, X. Gao, and L. Wang, "Reverse dispersion entropy: a new complexity measure for sensor signal," *Sensors*, vol. 23, no. 19, 2019.

[20] T. Tanaka and D. P. Mandic, "Complex empirical mode decomposition," *IEEE Signal Processing Letters*, vol. 14, no. 2, pp. 101–104, 2007.

[21] G. Rilling, P. Flandrin, P. Goncalves, and J. M. Lilly, "Bivariate empirical mode decomposition," *IEEE Signal Processing Letters*, vol. 14, no. 12, pp. 936–939, 2007.

[22] A. Hemakom, A. Ahrabian, D. Looney, N. u. Rehman, and D. P. Mandic, "Nonuniformly sampled trivariate empirical mode decomposition," in *Proceedings of the 2015 IEEE International Conference on Acoustics*, South Brisbane, QLD, Australia, April 2015.